

## Abstract

In time-distance helioseismology wave travel times are measured from the cross-correlation between Doppler velocities recorded at any two locations on the solar surface. All local helioseismology inferences rely critically on the definition of travel time and its accuracy. We compare two different methods to extract the travel times from the noisy cross-correlation functions. The first method consists of fitting a 5-parameter analytic function to the cross-correlation to obtain the phase travel time. The second method consists of linearizing the distance between the observed cross-correlation and a sliding reference cross-correlation (the only parameter is the travel time). We find that the one-parameter fits are more robust with respect to noise. Using SOHO data from the MDI Structure Program for the years 1996 - 2003, we study in detail the statistical properties of the noise associated with the travel-time measurements for the two different fitting methods.

## 1. INTRODUCTION

We implement two measurement techniques and compare them for robustness to solar noise. The first method consists of fitting a 5-parameter analytic function to the cross-correlation to obtain the phase travel time (Kosovichev & Duvall 1997). The second method consists of linearizing the distance between the observed cross-correlation and a sliding reference cross-correlation, where the only parameter is the travel time (Gizon & Birch 2004). This last method is motivated by studies in geophysics (Zhao & Jordan 1998). Here we use a set of velocity maps recorded every minute by the Michelson Doppler Imager (MDI) during the period 1996 - 2003 (SOHO/MDI Structure Program, Scherrer et al. 1995). This long time series of observations enables us to study in detail the statistical properties of the noise associated with the travel-time measurements for the two different fitting methods.

## 2. DATA

The analyzed data consists of medium- $l$  SOHO/MDI dopplergrams. The data reduction has been described by Giles (2000). Images are grouped into  $T = 72$  h periods for de-trending of solar rotation and supergranulation. Regions, spanning  $100^\circ$  in latitude  $\lambda$  and longitude were tracked at the Carrington rotation rate for the 72 h-period. The further processing included applying a high-pass filter at 1.7 mHz to remove the supergranulation signal. We then apply a filter to the data to remove the f-mode signal. Temporal cross-correlations  $C(t)$  were obtained by a code developed by Giles (2000) using pairs of points separated by an angular distance  $\Delta$  with orientation either north-south or east-west.

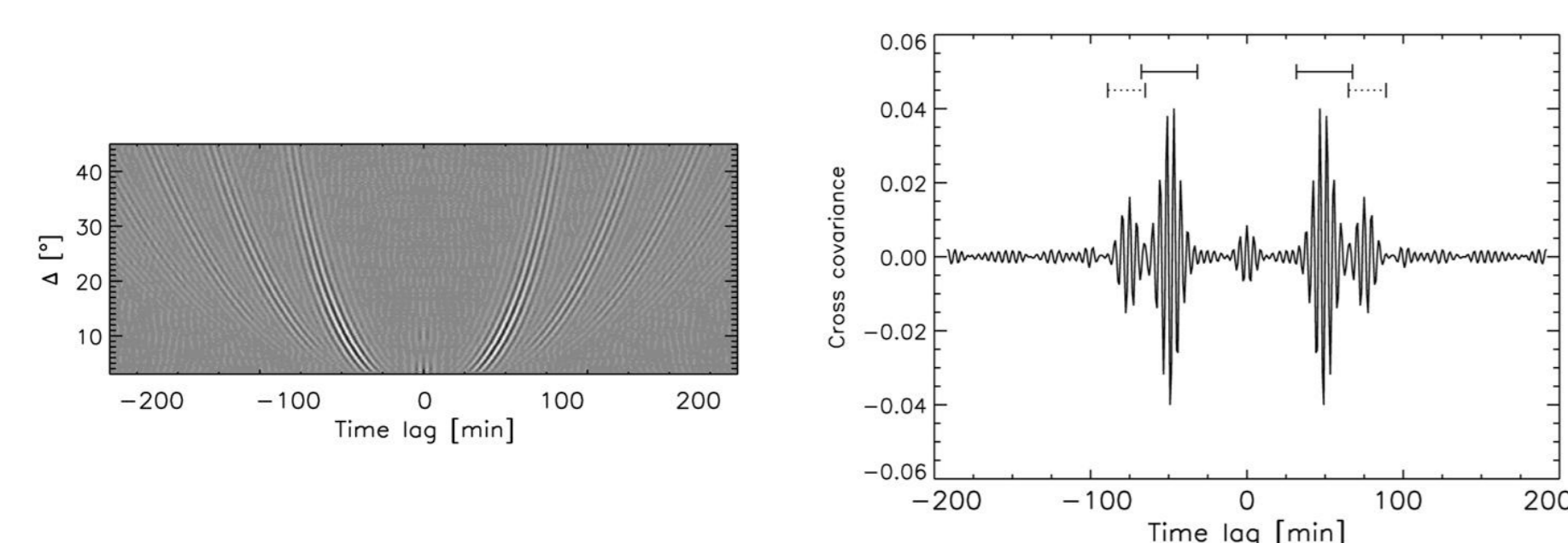


**Figure 1:** Left: North-south cross-covariances averaged over the period from May to July 1996 as a function of time lag and distance  $\Delta$ . Several ridges are visible in this plot. They correspond to the different bounces of the wave packets at the surface before reaching the distance  $\Delta$ . The first ridge with smallest time lag corresponds to the direct arrival of a wave packet. The other ridges correspond to wave packets that bounce off the surface once or more before reaching the distance  $\Delta$ . The signal-to-noise ratio at large distances is less. Right: Cut through the top diagram at  $\Delta = 10.5^\circ$ . The solid and dotted lines mark the fit ranges for the first and second bounces, respectively.

## 3. MEASURING TRAVEL TIMES

Here, we describe the two fitting techniques that are used to measure the travel times from the cross-covariances. We fit separately the first bounce and second bounce travel times as indicated in Fig. 2.

### 3.1 Gabor wavelet fitting

For each bounce, the cross-correlation can be approximated by a Gabor wavelet (Kosovichev & Duvall 1997)

$$C(t) = A^2 \cos(\omega_0(t + t_p)) e^{-(t-t_g)^2/2\sigma^2}$$

The five parameters are:  $A^2$ : amplitude,  $\omega_0$ : frequency,  $t_p$ : phase travel time,  $t_g$ : group travel time, and  $\sigma^2$ : width of Gaussian envelope. The group travel time  $t_g$  is given by the time lag of the peak of the envelope. The phase travel time  $t_p$  is defined as the modulo  $2\pi/\omega_0$ . In general  $t_p$  can be determined with higher accuracy than  $t_g$ . Note that the two branches of the cross-covariance are fitted separately. The corresponding phase travel times are denoted as  $t_{p+}$  for  $C(t > 0)$  and  $t_{p-}$  for  $C(t < 0)$ . In order to fit individual cross-covariances initial guesses for all the parameters are needed. Here we describe in detail the procedure that we use to determine these guesses. We use the long-term average cross-covariance shown in Fig. 1 to obtain initial guesses. As shown in Fig. 2 the guess for  $t_p$  is important because of the non-uniqueness of  $t_p$ . The guess for  $t_p$  is obtained iteratively. As a first step all phase travel-time measurements that are more than  $2\pi/\omega_0$  away from the initial guess are removed. Secondly, the remaining measurements of  $t_p$  are used to find the coefficients of a fifth-order polynomial to the phase time-distance relation (Chou & Duvall 2000). Thirdly, this fifth-order polynomial together with the original guesses for  $A^2$ ,  $\sigma^2$ ,  $\omega_0$  and  $t_g$  are used as new guesses for a further iteration of the Gabor-wavelet fit.

The procedure is repeated until the guesses converge. Figure 2 (right) shows phase travel-time measurements for the first and second bounce after five iterations. Once final guesses have been determined, the individual  $T = 72$  h cross-covariances can be fitted one at a time (see Fig. 2 for an example). Outliers in the  $t_p$  measurements may occur. By definition we call outliers measurements that lie 3 s away from the mean. We investigate the statistics of the travel-time measurements below.

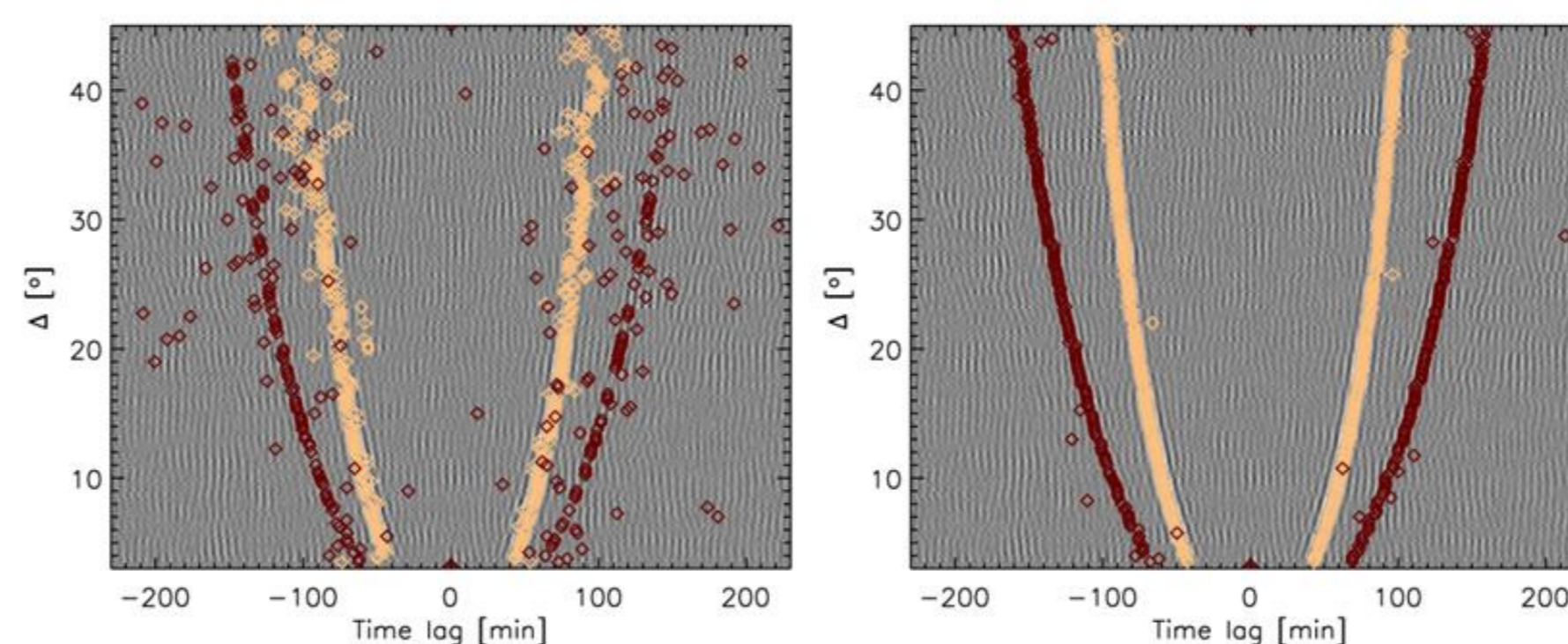


**Figure 2:** The time-distance diagram with phase travel-time measurements  $t_p$  for the first (yellow) and second (red) bounce in north-south data.  $T = 72$  h,  $\lambda = 0^\circ$ . Left: Phase travel-time measurements obtained by Gabor-wavelet fits with a rough guess for  $t_p$ . Right: Phase travel-time measurements obtained by Gabor-wavelet fits with a guess for  $t_p$  obtained after five steps of iterating the relation  $t_p(\Delta)$  by fifth-order polynomials.

### 3.2 One-parameter fit

Another approach of determining one-way travel-time measurements is to compare the observed cross-correlations with a sliding reference model  $C_{ref}$ . The reference cross-correlations are obtained by averaging the cross-correlation functions over 90 days (Fig. 1, left). The reference cross-covariance is shifted in time until it best resembles the data (Gizon & Birch 2002). The travel time is defined by:

$$\tau_{\pm} = \frac{\sum_i \mp f(\pm t_i) \dot{C}_{ref}(t_i) [C(t_i) - C_{ref}(t_i)]}{\sum_i f(\pm t_i) [\dot{C}_{ref}(t_i)]^2}$$

The window function  $f(t)$  selects the ridge of interest in the time-distance diagram. We denote by  $\tau_+$  the travel time for waves that move away from the starting location and by  $\tau_-$  the travel time for waves that move in the opposite direction. For each  $\lambda$  and  $\Delta$  we obtain a measurement of  $\tau_+$  and  $\tau_-$ . We note, in this procedure no fitting algorithm is involved. Therefore, convergence problems cannot occur. A travel-time measurement is always obtained.

## 4. COMPARISON OF THE TWO TECHNIQUES

Here we consider the travel-time differences. In the case of Gabor-wavelet fits these are given by  $t_{p+} - t_{p-}$ . In the case of the one-parameter fits these are  $\tau_+ - \tau_-$ . We compare the two measurement techniques. Both methods are affected by noise in the cross-covariances. We study the sensitivity of the two methods to this noise. Figure 3 shows travel-time shifts measured at the equator as a function of distance in north-south data. In general the two methods agree well. However, the Gabor-wavelet fitting produces outliers, even more frequently at large distances where the signal-to-noise ratio is worse. There the one-parameter fit still delivers results. We compare the distributions of travel-time shifts for all latitudes  $\lambda$ ; once for distances  $\Delta$  smaller than  $24^\circ$  and once for distances  $\Delta$  larger than  $24^\circ$  for one observing period of length  $T = 72$  h, cf. Fig. 4. The binning in the histograms is 10 s. There are 9667 travel-time measurements for  $\Delta < 24^\circ$  and 8036 measurements for  $\Delta > 24^\circ$ . We find in general for both methods a broader distribution for the larger distances. This is expected due to the fading signal with greater distances (cf. Fig. 1, left). Comparing the two measurement techniques the distribution for the Gabor-wavelet fit is always broader than the distribution for the one-parameter fit. The distribution of the one-parameter fit is Gaussian (Gizon & Birch 2004), whereas the distribution of the Gabor-wavelet fits has flat tails which shows that the distribution is not Gaussian.

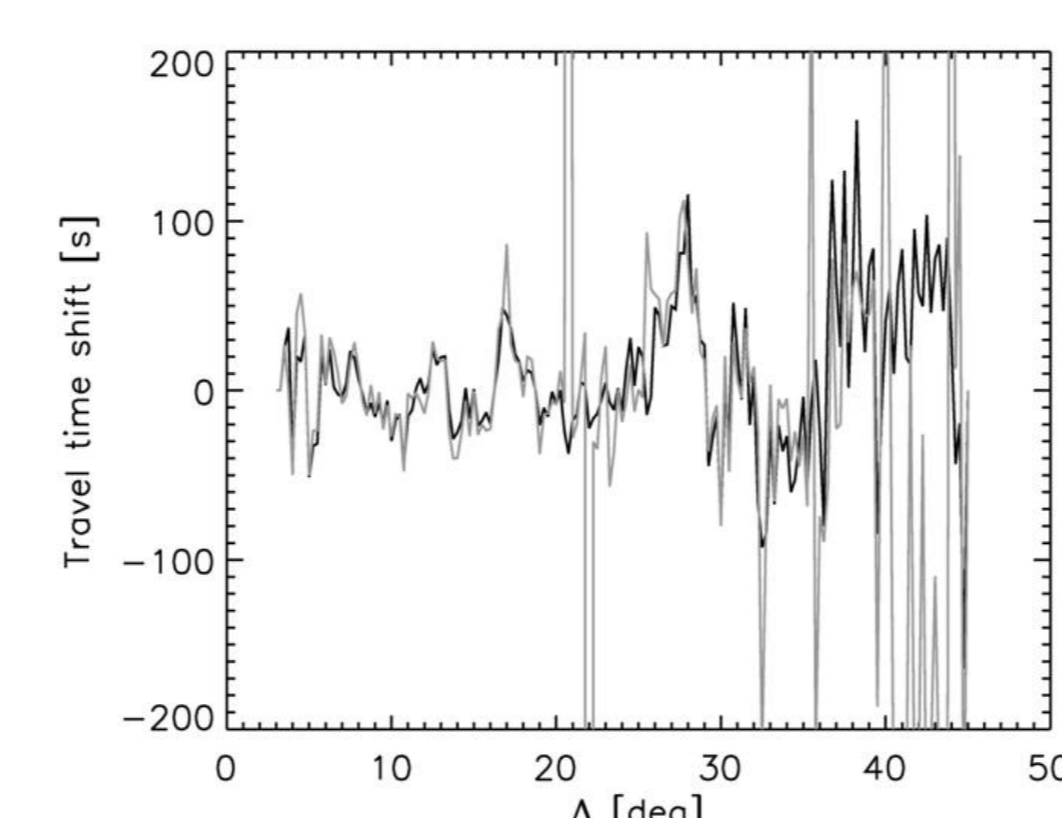


**Figure 3:** Travel-time differences at the equator for north-south data as a function of distance  $\Delta$ . Shown are results of the two measurement techniques Gabor-wavelet fit (grey) and one-parameter fit (black). Both measurements are obtained from the same cross-correlations. The observation time is 72 h.

All the measurements in the flat tails are suspected to be wrong. We note, that the Gabor-wavelet fit produces a non negligible amount of outliers. The number of outliers are indicated by arrows in the histograms. The relative number of outliers for  $\Delta < 24^\circ$  is 3.3%. The relative number of outliers for  $\Delta > 24^\circ$  is 9.2%. There are no outliers with the one-parameter fit.

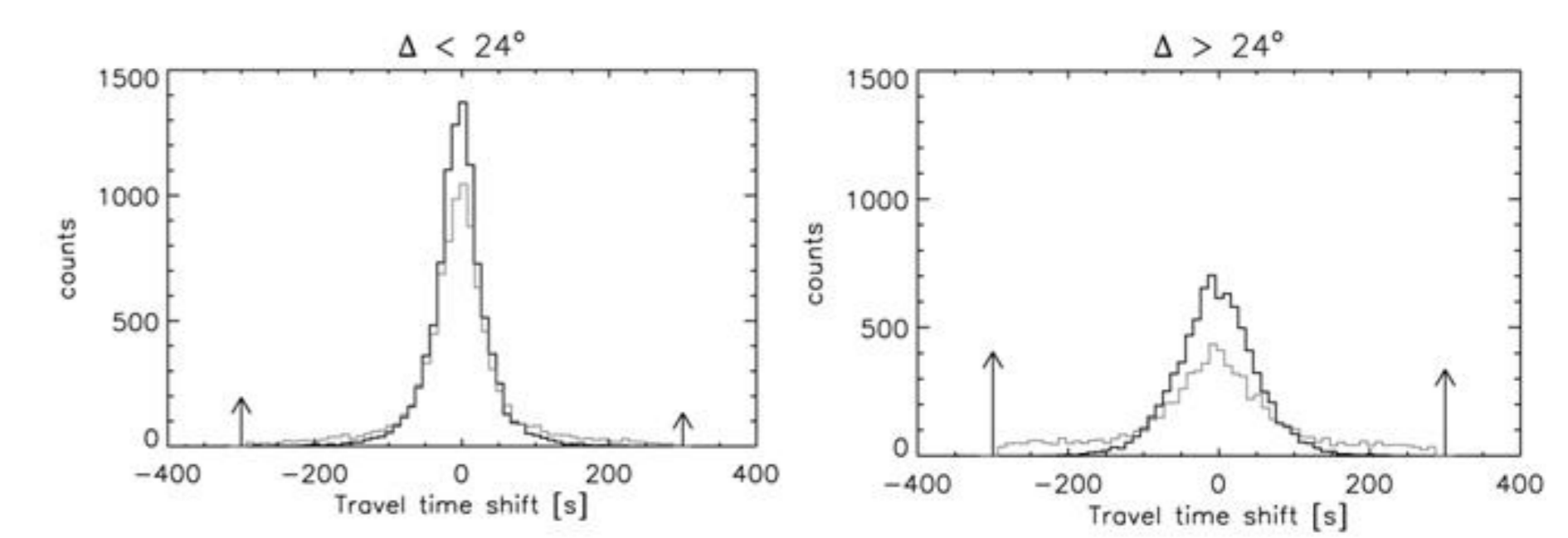


**Figure 4:** Histograms for travel-time shifts measured by the Gabor-wavelet fit (grey) and the one-parameter fit (black) applied to north-south data;  $T = 72$  h. Left: Measurements for distances lower than  $24^\circ$ . The total number of measurements is 9667. Right: Measurements for distances larger than  $24^\circ$ . The total number of measurements is 8036. In both cases the number of outliers produced by the Gabor-wavelet fit are indicated by arrows at the bins -300 s and 300 s, resp. The total number of outliers is 327 for  $\Delta < 24^\circ$  and 741 for  $\Delta > 24^\circ$ .

The signal-to-noise ratio in the cross-covariances varies strongly as a function of latitude  $\lambda$  and distance  $\Delta$ . This is mirrored in the travel-time measurements. Their standard deviation is also a function of  $\lambda$  and  $\Delta$  (cf., Fig. 5). The standard deviation is lowest  $\pm 20^\circ$  around the equator, i.e.  $\lambda = 0^\circ$ , and at distances around  $\Delta = 10^\circ$ . Towards higher latitudes and towards smaller and greater distances the noise is stronger. This result is comparable with results obtained by Giles (2000). In general, the one-parameter fit results in a lower variance of the measurements.

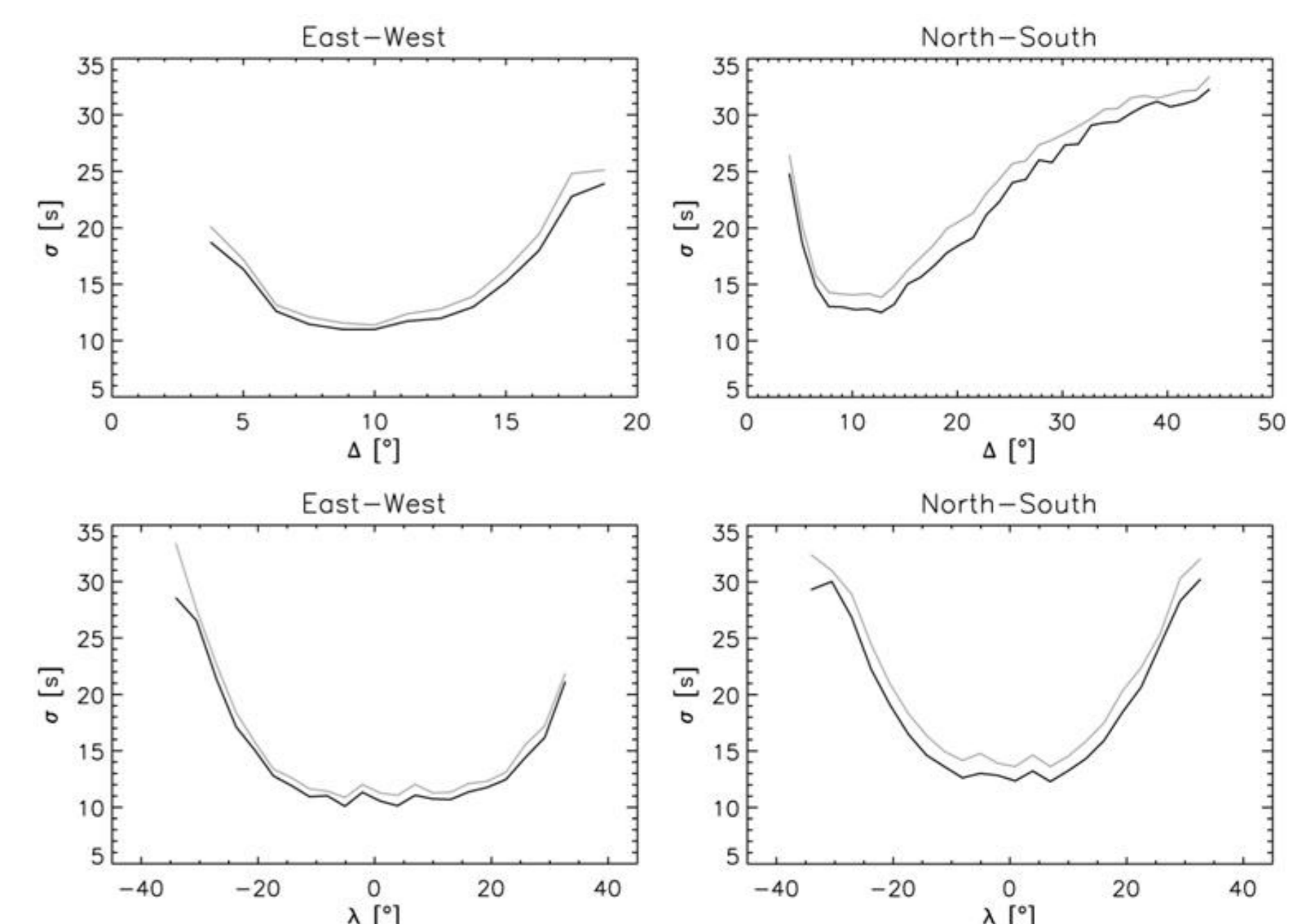


**Figure 5:** Standard deviation of east-west (left) and north-south (right) travel-time differences as a function of distance  $\Delta$  at the equator (top) and as a function of latitude  $\lambda$  at distance  $10^\circ$  (bottom). The travel-time differences were obtained using a Gabor-wavelet fit (grey) and the one-parameter fit (black) for  $T = 72$  h. Outliers in the Gabor-wavelet fits were removed. The results were binned over  $2.4^\circ$  degrees on the axes.

## 5. CONCLUSIONS

In general both methods agree well. The definition of travel time according to Gizon & Birch (2004) is robust to noise, because no fitting algorithm is involved. The distribution of the measurements is Gaussian in that case. The Gabor-wavelet fitting is not as robust and provides a non-Gaussian distribution of travel-time measurements. The variance of the measurements is a function of latitude and distance with a minimum at travel-distances around  $\Delta = 10^\circ$  and latitudes  $\pm 20^\circ$  around the equator. This finding agrees with the results obtained by Giles (2000). After removing the outliers returned by the Gabor-wavelet fits we find that the noise in the travel times is similar for both measurement methods. A full description of this work is given by Roth et al. (2007).

## References

- [1] Chou, D.-Y., Duvall, T.L., Jr., 2000, *ApJ* 533, 568
- [2] Giles, P., 2000, *PhD Thesis, Stanford Univ.*
- [3] Gizon, L., Birch, A.C., 2002, *ApJ* 571, 966
- [4] Gizon, L., Birch, A.C., 2004, *ApJ* 614, 472
- [5] Kosovichev, A., Duvall, T.L., Jr., 1997, in *SCORe 96*, p. 241
- [6] Roth, M., Gizon, L., Beck, J.G., 2007, *AN* 328, 215
- [7] Zhao, L., Jordan, T.H., 1998, *GeoJl* 133, 683